RESEARCH ACTIVITIES

Life and Coordination-Complex Molecular Science

Department of Life and Coordination-Complex Molecular Science is composed of two divisions of Biomolecular science, two divisions of Coordination molecular science and one adjunct division. Biomolecular science divisions cover the studies on the elucidation of functions and mechanisms for various types of sensor proteins, protein folding, molecular chaperone, and metal proteins. Coordination complex divisions undergo to develop molecular catalysts for the transformation of organic molecules, activation small inorganic molecules, and reversible conversion between chemical and electrical energies. Based on the fundamental researches conducted by each division, interdisciplinary alliances in the Department aim at the creation of fundamental concepts for the molecular and energy conversion.

Bioinorganic Chemistry of Novel Hemeproteins

Department of Life and Coordination-Complex Molecular Science
Division of Biomolecular Functions

AONO, Shigetoshi	Professor
YOSHIOKA, Shiro	Assistant Professor
SAWAI, Hitomi	IMS Fellow (–March '07)
	JSPS Post-Doctoral Fellow (April '07–)
YASUHIRA, Kengo	IMS Fellow
YOSHIMURA, Hideaki	Graduate Student*
NISHIMURA, Muneto	Graduate Student
TANIZAWA, Misako	Secretary

Heme-based sensor proteins show a novel function of the heme prosthetic group, in which the heme acts as the active site for sensing the external signal such as diatomic gas molecules and redox change. Aldoxime dehydratase is another novel hemeprotein, in which the heme prosthetic group tethers the substrate for its dehydration reaction. Our research interests are focused on the elucidation of the structure-function relationships of these novel hemeproteins.

1. Crystal Structure of CO-Sensing Transcription Activator CooA Bound to Exogenous Ligand Imidazole[1)]

CooA is a CO-dependent transcriptional activator and transmits a CO sensing signal to a DNA promoter that controls the expression of the genes responsible for CO metabolism. CooA contains a b-type heme as the active site for sensing CO. CO binding to the heme induces a conformational change that switches CooA from an inactive to an active DNA-binding form. Here, we report the crystal structure of an imidazole-bound form of CooA from *Carboxydothermus hydrogenoformans* (Ch-CooA). In the resting form, Ch-CooA has a six-coordinate ferrous heme with two endogenous axial ligands, the α-amino group of the N-terminal amino acid and a histidine residue. The N-terminal amino group, which is coordinated to the heme in CooA, is replaced by CO. This substitution presumably triggers a structural change leading to the active form. The crystal structure of Ch-CooA reveals that imidazole binds to the heme, which replaces the N terminus, as does CO. The dissociated N terminus is positioned approximately 16 Å from the heme iron in the imidazole-bound form. In addition, the heme plane is rotated by 30° about the normal of the porphyrin ring compared to that found in the inactive form of *Rhodospirillum rubrum* CooA. Even though the ligand exchange takes place, imidazole-bound Ch-CooA remains in the inactive form for DNA binding. These results indicate that the release of the N terminus resulting from imidazole binding is not sufficient to activate CooA. The structure provides new insights into the structural changes required to achieve activation.

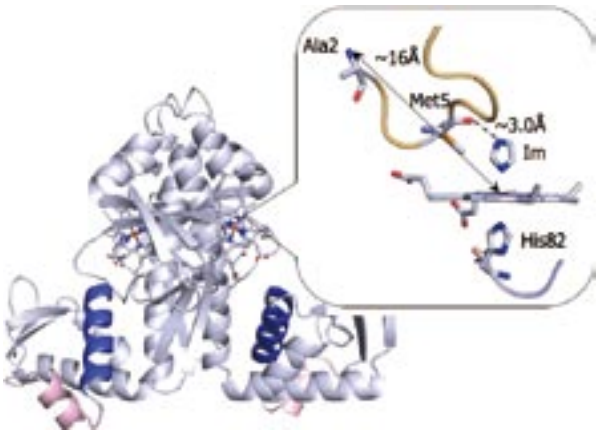

Figure 1. Structure of imidazole-bound Ch-CooA and the close-up view around the heme.

2. The Formation of Hydrogen Bond in the Proximal Heme Pocket of HemAT-Bs upon Ligand Binding[2)]

HemAT-Bs is the heme-based O_2 sensor responsible for aerotaxis control in *Bacillus subtilis*. In this study, we measured the time-resolved resonance Raman spectra of full-length HemAT-Bs wild-type (WT) and Y133F in the deoxy form and the photoproduct after photolysis of CO-bound form.

In WT, the ν_{Fe-His} band for the 10 ps photoproduct was observed at higher frequency by about 2 cm^{-1} compared with that of the deoxy form. This frequency difference is relaxed in hundreds of picoseconds. This time-dependent frequency shift would reflect the conformational change of the protein matrix. On the other hand, Y133F mutant does not show such a substantial ν_{Fe-His} frequency shift after photolysis. Since a hydrogen bond to the proximal His induces an up-shift of the ν_{Fe-His} frequency, these results indicate that Tyr133 forms a hydrogen bond to the proximal His residue upon the ligand binding. We discuss a functional role of this hydrogen bond formation for the signal transduction in HemAT-Bs.

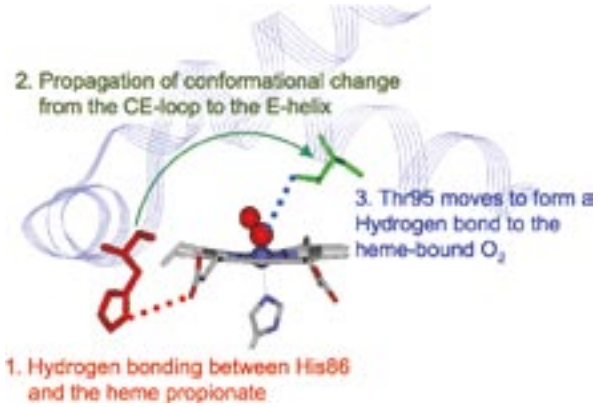

Figure 2. Signal transduction pathway of HemAT-Bs.

3. Two Ligand Binding Sites in the O_2-Sensing Signal Transducer HemAT: Implication for Ligand Recognition/ Discrimination and Signaling[3)]

We have identified a ligand (CO) accommodation cavity in the signal transducer sensor protein HemAT (heme-based aerotactic transducer) that allows us to gain single-molecule insights into the mechanism of gas sensor proteins. Specific mutations that are distal and proximal to the heme were designed to perturb the electrostatic field near the ligand that is bound to the heme and near the accommodated ligand in the cavity. We report the detection of a second site in heme proteins in which the exogenous ligand is accommodated in an internal cavity. The conformational gate that directs the ligand-migration pathway from the distal to the proximal site of the heme, where the ligand is trapped, has been identified. The data provide evidence that the heme pocket is the specific ligand trap and suggest that the regulatory mechanism may be tackled starting from more than one position in the protein. Based on the results, we propose a dynamic coupling between the two distinct binding sites as the underlying allosteric mechanism for gas recognition discrimination that triggers a conformational switch for signaling by the oxygen sensor protein HemAT.

4. Systematic Regulation of the Enzymatic Activity of Phenylacetaldoxime Dehydratase by Exogenous Ligand[4)]

Phenylacetaldoxime dehydratase from *Bacillus* sp. OxB-1 (OxdB) contains a heme that acts as the active site for the dehydration reaction of aldoxime. Ferrous heme is the active form, in which the heme is 5-coordinated with His282 as the proximal ligand. In this work, we evaluated the functional role of the proximal ligand for the catalytic properties of the enzyme by "the cavity mutant technique." H282G mutant of OxdB lost the enzymatic activity, though the heme, which was 5-coordinated with a water (or OH^-) as an axial ligand, existed in the protein matrix. The enzymatic activity was rescued by imidazole or pyridine derivatives that acted as the exogenous proximal ligand. By changing electron donation ability of these exogenous ligands with different substituents, the enzymatic activity could be regulated systematically. The stronger electron donation ability of the exogenous ligand, the higher restored enzymatic activity. Interestingly, H282G OxdB with 2-methyl imidazole showed a higher activity than wild type enzyme. Kinetic analyses revealed that the proximal His regulated not only the affinity of the substrate binding to the heme but the elimination of the OH group from the substrate.

References

1) H. Komori, S. Inagaki, S. Yoshioka, S. Aono and Y. Higuchi, *J. Mol. Biol*. **367**, 864–871 (2007).
2) H. Yoshimura, S. Yoshioka, Y. Mizutani and S. Aono, *Biochem. Biophys. Res. Commun*. **357**, 1053–1057 (2007).
3) E. Pinakoulaki, H. Yoshimura, V. Daskalakis, S. Yoshioka, S. Aono and C. Varotsis, *Proc. Natl. Acad. Sci. U.S.A.* **103**, 14796–14801 (2006).
4) K. Kobayashi, M. Kubo, S. Yoshioka, T. Kitagawa, K. Kato, Y. Asano and S. Aono, *ChemBioChem* **7**, 2004–2009 (2006).

* Present Address; Kyoto University, Kyoto 606-8501

Elucidation of the Molecular Mechanisms of Protein Folding

Department of Life and Coordination-Complex Molecular Science
Division of Biomolecular Functions

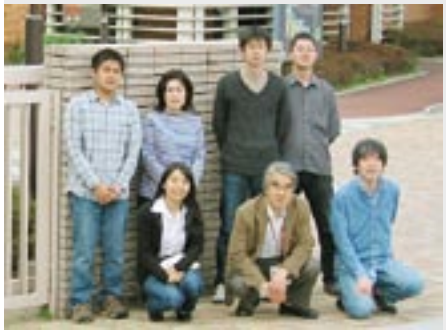

KUWAJIMA, Kunihiro	Professor
CHAUDHURI, Tapan K.	Visiting Associate Professor
MAKI, Kosuke	Assistant Professor*
MUKAIYAMA, Atsushi	IMS Fellow
VOLETY, Srinivas	Visiting Scientist; JSPS Invited Fellow
NAKAMURA, Takashi	Post-Doctoral Fellow
MIZUKI, Hiroko	Research Fellow
TAKAHASHI, Kazunobu	Graduate Student†
ISOGAI, Miho	Secretary

Kuwajima group is studying mechanisms of *in vitro* protein folding and mechanisms of molecular chaperone function. Our goal is to elucidate the physical principles by which a protein organizes its specific native structure from the amino acid sequence. In this year, we studied the equilibrium and kinetics of canine milk lysozyme folding/unfolding by peptide and aromatic circular dichroism and tryptophan fluorescence spectroscopy, and the unfolding pathways of goat α-lactalbumin by high-temperature molecular dynamics simulations.

1. Equilibrium and Kinetics of the Folding and Unfolding of Canine Milk Lysozyme[1)]

The equilibrium and kinetics of canine milk lysozyme folding/unfolding were studied by peptide and aromatic circular dichroism and tryptophan fluorescence spectroscopy. The Ca^{2+}-free apo form of the protein exhibited a three-state equilibrium unfolding, in which the molten globule state is well populated as an unfolding intermediate. A rigorous analysis of holo protein unfolding, including the data from the kinetic refolding experiments, revealed that the holo protein also underwent three-state unfolding with the same molten globule intermediate. Although the observed kinetic refolding curves of both forms were single-exponential, a burst-phase change in the peptide ellipticity was observed in both forms, and the burst-phase intermediates of both forms were identical to each other with respect to their stability, indicating that the intermediate does not bind Ca^{2+}. This intermediate was also shown to be identical to the molten globule state observed at equilibrium. The Φ-value analysis, based on the effect of Ca^{2+} on the folding and unfolding rate constants, showed that the Ca^{2+}-binding site was not yet organized in the transition state of folding. A comparison of the result with that previously reported for α-lactalbumin indicated that the folding initiation site is different between canine milk lysozyme and α-lactalbumin, and hence, the folding pathways must be different between the two proteins. These results thus provide an example of the phenomenon wherein proteins that are very homologous to each other take different folding pathways. It is also shown that the native state of the apo form is composed of at least two species that interconvert.

2. Unfolding Pathways of Goat α-Lactalbumin as Revealed in Multiple Alignment of Molecular Dynamics Trajectories[2)]

Molecular dynamics simulations of protein unfolding were performed at an elevated temperature for the authentic and recombinant forms of goat α-lactalbumin. Despite very similar three-dimensional structures, the two forms have significantly different unfolding rates due to an extra N-terminal methionine in the recombinant protein. To identify subtle differences between the two forms in the highly stochastic kinetics of unfolding, we classified the unfolding trajectories using the multiple alignment method based on the analogy between the biological sequences and the molecular dynamics trajectories. A dendrogram derived from the multiple trajectory alignment revealed a clear difference in the unfolding pathways of the authentic and recombinant proteins, *i.e.* the former reached the

transition state in an all-or-none manner while the latter unfolded less cooperatively. It was also found in the classification that the two forms of the protein shared a common transition state structure, which was in excellent agreement with the transition state structure observed experimentally in the Φ-value analysis.

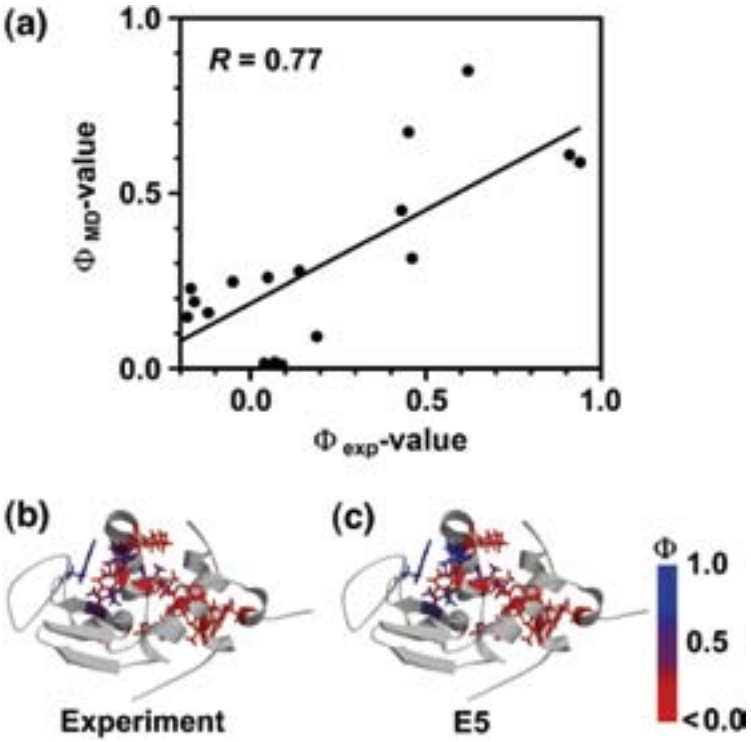

Figure 1. (a) Scatter plot showing the correlation between Φ_{exp} and Φ_{MD} of recombinant goat α-lactalbumin; Φ_{exp} contains small negative values, and Φ_{MD} was calculated for the structures around the center of cluster E5. (b) Φ_{exp} and (c) Φ_{MD} mapped onto the three-dimensional structure of goat α-lactalbumin.

References

1) H. Nakatani, K. Maki, K. Saeki, T. Aizawa, M. Demura, K. Kawano, S. Tomoda and K. Kuwajima, *Biochemistry* **46**, 5238–5251 (2007).

2) T. Oroguchi, M. Ikeguchi, M. Ota, K. Kuwajima and A. Kidera, *J. Mol. Biol.* **371**, 1354–1364 (2007).

* Present Address; Department of Physics, Nagoya University, Chikusa-ku, 464-8602 Nagoya

† carrying out graduate research on Cooperative Education Program of IMS with the University of Tokyo

Structure-Function Relationship of Metalloproteins

Department of Life and Coordination-Complex Molecular Science
Division of Biomolecular Functions

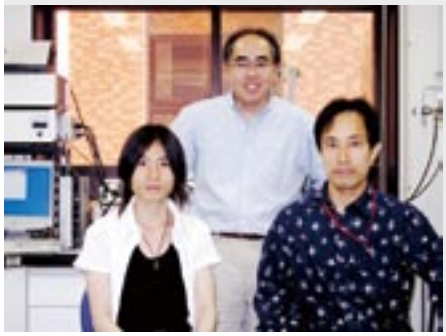

FUJII, Hiroshi	Associate Professor
KURAHASHI, Takuya	Assistant Professor
KUJIME, Masato	Post-Doctoral Fellow*
TAKAHASHI, Akihiro	Graduate Student
TANIZAWA, Misako	Secretary

Metalloproteins are a class of biologically important macromolecules, which have various functions such as oxygen transport, electron transfer, oxidation, and oxygenation. These diverse functions of metalloproteins have been thought to depend on the ligands from amino acid, coordination structures, and protein structures in immediate vicinity of metal ions. In this project, we are studying the relationship between the electronic structures of the metal active sites and reactivity of metalloproteins.

1. A Trigonal-Bipyramidal Geometry Induced by an External Water Ligand in a Sterically Hindered Iron Salen Complex, Related to the Active Site of Protocatechuate 3,4-Dioxygenase[1)]

A unique distorted trigonal-bipyramidal geometry observed for the nonheme iron center in protocatechuate 3,4-dioxygenase (3,4-PCD) was carefully examined utilizing a sterically hindered iron salen complex, which well reproduces the endogenous His_2Tyr_2 donor set with water as an external ligand (Figure 1). X-ray crystal structures of a series of iron model complexes containing bis(3,5-dimesitylsalicylidene)-1,2-dimesitylethylenediamine indicate that a distorted trigonal-bipyramidal geometry is achieved upon binding of water as an external ligand. The extent of a structural change of the iron center from a preferred square-pyramidal to a distorted trigonal-bipyramidal geometry varies with the external ligand that is bound in the order Cl << EtO < H_2O, which is consistent with the spectrochemical series. The distortion in the model system is not due to steric repulsions, but electronic interactions between the external ligand and the iron center, as evidenced from the X-ray crystal structures of another series of iron model complexes with a less-hindered bis(3-xylylsalicylidene)-1,2-dimesitylethylenediamine ligand, as well as by DFT calculations. Further spectroscopic investigations indicate that a unique distorted trigonal-bipyramidal geometry is indeed maintained even in solution. The present model study provides a new viewpoint that a unique distorted trigonal-bipyramidal iron site might not be preorganized by a 3,4-PCD protein, but could be electronically induced upon the binding of an external hydroxide ligand to the iron(III) center. The structural change induced by the external water ligand is also discussed in relation to the reaction mechanism of 3,4-PCD.

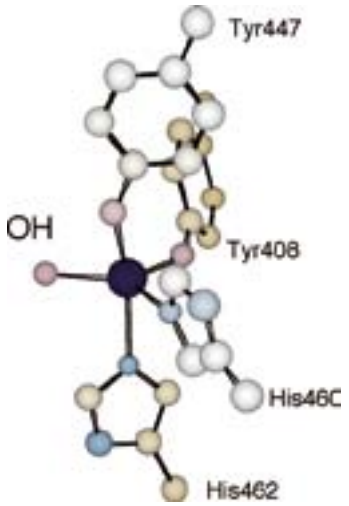

Figure 1. Active site structure of Protocatechuate 3,4-dioxygenase.

2. ^{63}Cu NMR Spectroscopy of Copper(I) Complexes with Various Tridentate Ligands: CO as a Useful ^{63}Cu NMR Probe for Sharpening ^{63}Cu NMR Signals and Analyzing the Electronic Donor Effect of a Ligand[2)]

^{63}Cu NMR spectroscopic studies of copper(I) complexes with various N-donor tridentate ligands, shown in Figure 1, are reported. As has been previously reported for most copper(I) complexes, ^{63}Cu NMR signals, when acetonitrile is coordi-

nated to copper(I) complexes of these tridentate ligands, are extremely broad or undetectable. However, when CO is bound the above tridentate copper(I) complexes, the ^{63}Cu NMR signals become much sharper and show a large downfield shift, compared to those for the corresponding acetonitrile complexes. Temperature dependence of ^{63}Cu NMR signals for these copper(I) complexes show that a quadrupole relaxation process is much more significant to their ^{63}Cu NMR line widths than a ligand exchange process. Therefore, an electronic effect of the copper bound CO makes the ^{63}Cu NMR signal sharp and easily detected. The large downfield shift for the copper(I) carbonyl complex can be explained by a paramagnetic shielding effect induced by the copper bound CO, which amplifies small structural and electronic changes that occur around the copper ion to be easily detected in their ^{63}Cu NMR shifts. This is evidenced by the correlation between the ^{63}Cu NMR shifts for the copper(I) carbonyl complexes and their ν(C≡O) values. Furthermore, the ^{63}Cu NMR shifts for copper(I) carbonyl complexes with imino type tridentate ligands show a different correlation line with those for amino type tridentate ligands. On the other hand, ^{13}C NMR shifts for the copper bound ^{13}CO for these copper(I) carbonyl complexes do not correlate with the ν(C≡O) values. The X-ray crystal structures of these copper(I) carbonyl complexes do not show any evidence of a significant structural change around the Cu–CO moiety. The findings herein show that CO has great potential as a probe in ^{63}Cu NMR spectroscopic studies for characterizing the nature of the environment around copper ions in copper complexes.

3. Activation Parameters for Cyclohexene Oxygenation by Oxoiron(IV) Porphyrin π-Cation Radical Complex: Entropy Control of Allylic Hydroxylation Reaction[3)]

Cytochromes P450 (P450) are very versatile catalysts, which activate molecular oxygen and catalyze hydrocarbon hydroxylation or alkene epoxidation with high stereoselectivity. Reaction of P450 with cyclohexene yields a mixture of two major products: cyclohexene oxide (an epoxidation product) and 2-cyclohexen-1-ol (an allylic hydroxylation product). Interestingly, the ratio of epoxidation to allylic hydroxylation products, *i.e.*, the chemoselectivity, is changed by P450 isozymes and by mutation of a single amino acid near the proximal or distal side. In addition, P450 model studies using synthetic iron porphyrin complexes showed that the chemoselectivity depends on various other factors, such as the nature of the porphyrin and axial ligands, solvents, and reaction temperature. While these enzymatic and model studies suggest that chemoselectivity is dependent on the electronic structure of the reactive intermediate, oxoiron(IV) porphyrin π-cation radical species (compound I), it is not clear how compound I controls chemoselectivity. Recently, the reaction mechanism and chemoselectivity of P450 have been studied by theoretical calculations based on density functional theory (DFT). In DFT studies, reaction mechanism and chemoselectivity are predicted from calculated activation energy, E_a, for epoxidation and allylic hydroxylation reactions of oxoiron(IV) porphyrin π-cation radical species. These studies are based on the assumption that the contribution of entropy of activation, $\Delta S^{\ddagger}$, is much smaller than that of enthalpy of activation, $\Delta H^{\ddagger}$. However, the validity of this assumption remains unproven because the activation parameters for epoxidation and allylic hydroxylation reactions of compound I species are yet to be determined. To better understand epoxidation and allylic hydroxylation reactions, the present study ascertained the activation parameters for epoxidation and allylic hydroxylation reactions of cyclohexene with compound I species, $Fe^{IV}O$ $(TMP)^{+\bullet}Cl$ (**1**), (Figure 2). This study demonstrated that epoxidation is an enthalpy-controlled reaction, while allylic hydroxylation is an entropy-controlled reaction. The large contribution of the entropy term, $-T\Delta S^{\ddagger}$, to the free energy of activation, $\Delta G^{\ddagger}$, indicated that $\Delta G^{\ddagger}$, rather than E_a, should be used to predict reaction mechanisms and chemoselectivity.

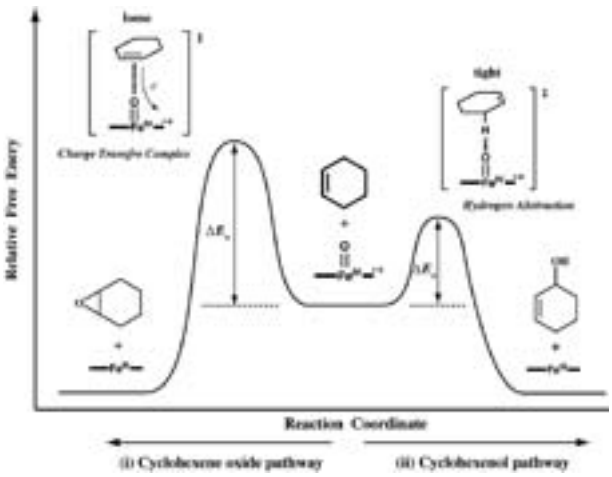

Figure 2. A cartoon of the reaction coordinates for allylic hydroxylation and epoxidation of cyclohexene by oxoiron(IV) porphyrin π-cation radical complex.

References

1) T. Kurahashi, K. Oda, M. Sugimoto, T. Ogura and H. Fujii, *Inorg. Chem.* **45**, 7709–7721 (2006).
2) M. Kujime, T. Kurahashi, M. Tomura and H. Fujii, *Inorg. Chem.* **46**, 541–551 (2007).
3) A. Takahashi, T. Kurahashi and H. Fujii, *Inorg. Chem.* **46**, 6227–6229 (2007).

Award

TAKAHASHI, Akihiro; Award for Oral Presentation by Graduate Student in Annual Meeting of Chemical Society of Japan.

* Present Address; Advanced Industrial Science and Technology, Tsukuba 305-8565

Fabrication of Silicon-Based Planar Ion-Channel Biosensors and Integration of Functional Cell Membrane Model Systems on Solid Substrates

Department of Life and Coordination-Complex Molecular Science
Division of Biomolecular Sensing

URISU, Tsuneo	Professor
TERO, Ryugo	Assistant Professor
MAO, Yangli	IMS Fellow
CHIANG, Tsung-Yi	Research Fellow
UNO, Hidetaka	Graduate Student
ZHANG, Zhen-Long	Graduate Student
SAYED, Abu	Graduate Student
NAKAI, Naohito	Graduate Student
ASANO, Toshifumi	Graduate Student
SHIMIZU, Atsuko	Secretary

To combining the human brain and the supercomputer is a dream of the scientist. To realize this dream we must develop several interface devices which can pick up several signals from neural cells such as electrical, optical and molecular signals. We run two main projects targeting the reactions on cell membranes. One is the fabrication of Si-based ion-channel biosensor, which is one of the above interface device to detect the neurotransmitter molecules. The other is the fundamental understanding of bilayer membrane properties using the artificial lipid bilayers on solid substrates, which is called supported bilayers, by means of atomic force microscope and fluorescence microscope-based techniques.

1. Supported Planar Lipid Bilayers on Step-and-Terrace TiO_2 Surfaces

We studied the influence of substrate surface properties on supported planar bilayer (SPB) using atomic force microscope and fluorescence microscope. Effects of surface hydrophilicity and atomic structures on the SPB formation process, morphology, and phase-separation were investigated on single-step-and-terrace rutile-TiO_2 low index surfaces. Step-and-terrace surfaces of rutile-TiO_2 (100), (110) and (001) were formed by etching in 10% HF *aq*. and annealing at O_2 flow (1.0 L min^{-1}) at 700–850 °C. Figure 1a shows the step-and-terrace TiO_2(100) surface. The height of each step was 0.25 nm, that corresponded to the height of the TiO_2(100) unit cell. Flat and continuous SPB was formed on both TiO_2 (100) and (001) surfaces by the vesicle fusion method. The dipalmitoleoylphosphatidylcholine (DPoPC)-SPB on the single- and double-step TiO_2(100) had a ratchet-like structure following the step-and-terrace structure of the substrate, but that on the half-step TiO_2(001) did not have the morphology reflecting the substrate structure. The atomic steps on the TiO_2(100) substrate affected the domain shapes in the binary bilayer of DPoPC and dipalmitoylphosphatidylcholine (DPPC). Some of the gel-phase domain (DPPC-rich) edges on the step-and-terrace TiO_2(100) surface run along the atomic step on the substrate (Figure 1b). This results shows the only 0.25 nm atomic structure on the substrate definitely affects to the lateral lipid assembly in several hundreds nanometer scale.

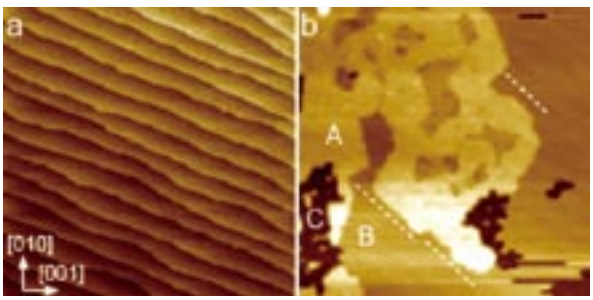

Figure 1. (a) AFM image (2.0×2.0 μm^2) of the step-and-terrace TiO_2(100) surface. The image was obtained in air. (b) AFM image (2.0×2.0 μm^2) of the DPoPC+DPPC binary bilayer on the TiO_2(100). The regions with the brightest (A), middle (B) and darkest (C) contrast are gel-phase domain, liquid crystal domain and defects (bare TiO_2), respectively. The dotted line represent the direction of the substrate atomic step. The image was obtained in a buffer solution.

2. Analysis of Alzheimer's Disease Pathogenesis by *in situ* AFM

Alzheimer's disease (AD) is one of the most common age-associated pathologies, which inevitably leads to dementia and death. Amyloid plaques and neurofibrillary tangles containing beta-amyloid (Aβ) are two of the pathological hallmarks of AD. A key event in AD pathogenesis is the conversion of Aβ peptide from soluble to toxic aggregation in the brain. In particular, how to aggregate and interact with lipid membranes is one of the most important researches because the membrane

surface might be responsible for both neurotoxicity and senile plaque formation.

Supported planar bilayers (SPBs) are useful *in vitro* mimicking system for natural biological membranes. Recently, several reports showed that these inert substrates affected to the SPB fluidity, phase-transition, formation rate, and domain structures. Detailed substrate effects of such systems are of paramount importance for SPBs to mimic cell membranes successfully and for the design of new applications in biosensors and surface bio-functionalization.

In this study, we investigated the interaction of Aβ40-GM1 on the ternary-SPB of Ganglioside (GM1), sphingomyelin (SM) and cholesterol (Chol), which is used as the natural membrane raft, by AFM, fluorescence microscopy, and CTX-B and Thioflavin T assay. The novel phase- separations with triangle domains are observed on mica surface by AFM (Figure 2a), whereas the second bilayers were formed on SiO_2 substrate at the same conditions (Figure 2b).

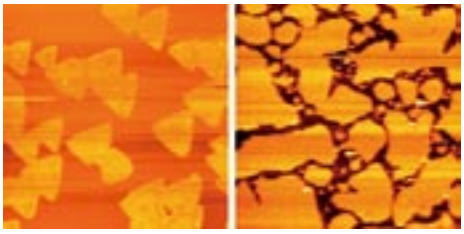

Figure 2. (a, b) AFM images of GM1/SM/Chol (20:40:40 molar ratio)-SPBs on mica (a: 10×10 μm^2) and SiO_2 (b: 5.0×5.0 μm^2) substrates.

3. Fabrication of Si-Based Planar Type Patch Clamp Biosensor Using Silicon on Insulator Substrate[1)]

The aim of this study is to fabricate the planar type patch clamp ion-channel biosensor, which can detect the neurotransmitter molecules, using silicon-on-insulator (SOI) substrate. The micropore with 1.2 μm diameter was formed through the top Si layer and the SiO_2 box layer of the SOI substrate by focused ion beam (FIB). Then the substrate is assembled into the microfluidic circuit. The human embryonic kidney 293 (HEK-293) cell transfected with transient receptor potential vanilloid type 1 (TRPV1) was positioned on the micropore and the whole-cell configuration was formed by the suction. We succeeded to measure the capsaicin-induced Ca^{2+} cannel current of the TRPV1 (Figure 3), when we added capsaicin to the extracellular solution as a ligand molecule. The channel current showed the desensitization unique to the TRPV1.

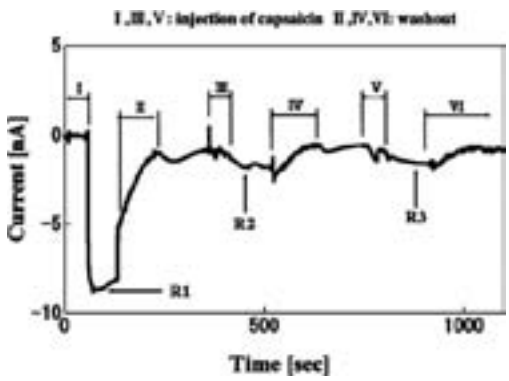

Figure 3. Whole-cell current of TRPV1-transfected HEK-293 cell activated by repeated capsaicin (7.1 μM) applications, which shows desensitization in the extracellular solution containing Ca^{2+}. The holding voltage was –30 mV.

4. Synchrotron Radiation Stimulated XeF_2 Etching Beam-Line with Focusing to Differential Pumping Pinhole

In the synchrotron radiation (SR) etching using XeF_2 gas, a high etching rate in addition to the unique characteristics of anisotropic etching and material selectivity is expected. We constructed a system for the SR-induced dry etching of Si using XeF_2 as etching gas in UVSOR. However, in the previous XeF_2 SR etching experiments, LiF_2 windows have been used at the beam entrance to the etching chamber to protect the upper stream part of the beam line from the corrosive XeF_2 gas. Due to the significant absorption of irradiation beam by this LiF_2 window and its rapid radiation damage, it was difficult to obtain a practical etching rate. Based on these our experiences, we have constructed a new XeF_2 etching beam line with expected high etching rate at UVSOR beam line 4A (Figure 4). The second focusing deflecting mirror (f = 2 mm) was set at 406cm down stream position from the first bent cylindrical pre-mirror. The pinhole (1 mm in diameter, 10 mm in length) is set at this second mirror focusing point. The sample surface position is 5 mm down-stream from this pinhole. The second mirror chamber is pumped by turbo-molecular pump (0.48 m^3 s^{-1}). And the sample chamber is pumped (4 × 10^{-4} m^3 s^{-1}) through XeF_2 gas line by rotary pump. According to this pinhole, sufficiently high vacuum (~10^{-4} Torr) in the second mirror chamber to protect the mirror from the contamination damage is kept with realizing a quite high XeF_2 gas pressure and high photon flux in the reaction chamber.

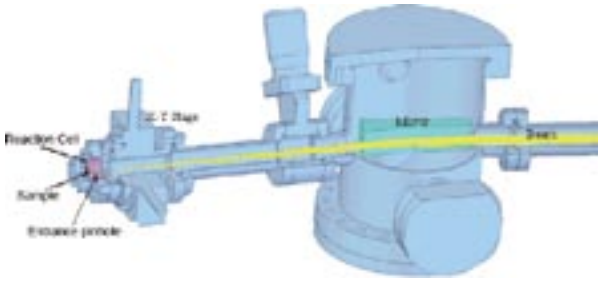

Figure 4. Schematic view of the etching chamber, pinhole and second focusing mirror.

Reference

1) Z. L. Zhang, T. Asano, H. Uno, R. Tero, M. Suzui, S. Nakao, T. Kaito, K. Shibasaki, M. Tominaga, Y. Utsumi, Y. L. Gao and T. Urisu, *Thin Solid Films* in press.

Development of Fluorescent and Bioluminescent Proteins for Imaging Biomolecules

Department of Life and Coordination-Complex Molecular Science
Division of Biomolecular Sensing

OZAWA, Takeaki	Associate Professor
TAKEUCHI, Masaki	Assistant Professor
HIDA, Naoki	IMS Fellow
MUHAMMAD, Awais	Post-Doctoral Fellow

Current focus on biological research is to quantify and image biomolecules in living cells and animals. To probe biomolecular functions and dynamics, we are exploring a new way for developing fluorescent and bioluminescent reporter proteins based on protein splicing and complementation techniques. The reporter proteins can be applied to development of analytical methods for detecting protein-protein interactions, intracellular localization of proteins and their dynamics, enzyme activities, gene expression and production of small biomolecules.

1. Imaging Dynamics of Endogenous Mitochondrial RNA in Single Living Cells

Location of cytoplasmic mRNA directs proteins to particular intracellular compartments, thereby controlling local cellular functions. Distinct localization of mitochondrial RNA (mtRNA) and the molecular mechanism are, however, poorly understood. We developed genetically-encoded RNA probes for characterizing localization and dynamics of mtRNA in single living cells. The probes consist of two RNA-binding domains of PUMILIO1, each connected with split fragments of a fluorescent protein capable of reconstituting upon binding to a target RNA. We designed the probes to specifically recognize a 16-base sequence of mtRNA encoding NADH dehydrogenase subunit 6 (ND6) and to be targeted into mitochondrial matrix, which allowed real-time imaging of ND6 mtRNA localization in living cells. We showed that ND6 mtRNA is localized within mitochondria and concentrated particularly on mtDNA. Movement of the ND6 mtRNA is restricted but oxidative stress with H_2O_2 induces the mtRNA to diffuse in mitochondria, and the mtRNA gradually decomposed thereafter. The present observation of mtRNA demonstrates that the RNA probes provide a means to understand mtRNA dynamics controlled both temporally and spatially in intracellular compartments in living cells.

2. A Genetically Encoded Optical Probe for Detecting Release of Proteins from Mitochondria toward Cytosol in Living Cells and Animals

We developed a genetically encoded bioluminescence indicator for monitoring the release of proteins from mitochondria in living cells. The principle of this method is based on reconstitution of split *Renilla reniformis* luciferase (Rluc) fragments by protein splicing with an Ssp DnaE intein. A target mitochondrial protein connected with an N-terminal fragment of Rluc and an N-terminal fragment of DnaE is expressed in mammalian cells. If the target protein is released from the mitochondria toward the cytosol upon stimulation with a specific chemical, the N-terminal Rluc meets the C-terminal Rluc connected with C-terminal DnaE in the cytosol, and thereby, the full-length Rluc is reconstituted by protein splicing. The extent of release of the target fusion protein is evaluated by measuring activities of the reconstituted Rluc. To test the feasibility of this method, we monitored the release of a Smac/DIABLO protein from mitochondria during apoptosis in living cells and mice. The present method allowed high-throughput screening of an apoptosis-inducing reagent, staurosporine, and imaging of the Smac/DIABLO release in cells and in living mice. This rapid analysis can be used for

screening and assaying chemicals that would increase or inhibit the release of mitochondrial proteins in living cells and animals.

3. Nongenomic Activity of Ligands in the Association of Androgen Receptor with Src

Androgen receptor (AR) induces cell proliferation by increasing the kinase activity of Src. We developed an approach for discriminating agonist and antagonist in a nongenomic steroid-signaling pathway using an association of AR with Src. We constructed a pair of genetically encoded indicators, where N- and C-terminal fragments of split firefly luciferase (FLuc) were fused to AR and Src, respectively. The fusion proteins with AR and Src are localized in the cytoplasm and on the plasma membrane, respectively. Upon being activated with androgen, AR undergoes an intramolecular conformational change and binds with Src. The association causes the complementation of the split FLuc and recovery of FLuc activity. The resulting luminescence intensities were taken as a measure of the rapid hormonal activity of steroids in the nongenomic AR signaling. Ten minutes were required for the AR-Src association by 5alpha-dihydroxytestosterone (DHT), which was completely inhibited by an antagonist, cyproterone acetate. The activities of ligands in the nongenomic pathway of AR were compared with those in the genomic pathway obtained on the basis of the nuclear trafficking of AR in mammalian cells. The comparison revealed that DHT and testosterone activate both genomic and nongenomic pathways of AR. 17beta-Estradiol and progesterone were found to be specific activators only for the genomic signaling pathway of AR. On the other hand, procymidone exhibited a specific activity only for the nongenomic signaling pathway of AR. The present approach is the first example addressing the agonistic and antagonistic activities of ligands in a nongenomic pathway of AR.

4. Cyclic Luciferase for Real-Time Sensing of Caspase-3 Activities in Living Mammals

Programmed cell death (apoptosis) is a crucial process involved in pathogenesis and progression of diseases, which is executed by Cysteine Aspartyl Proteases (caspases). The caspase activities in living subjects and their regulation with small chemical compounds are of great interest for screening drug candidates or pathological agents. We developed a genetically encoded bioluminescent indicator for high-throughput sensing and noninvasive real-time imaging of caspase activities in living cells and animals. Firefly luciferase connected with a substrate sequence of caspase-3 (Asp-Glu-Val-Asp) is cyclized by an intein DnaE (a catalytic subunit of DNA polymerase III). When the cyclic luciferase is expressed in living cells, the luciferase activity greatly decreases due to a steric effect. If caspase-3 is activated in the cells, it cleaves the substrate sequence embedded in the cyclic luciferase and the luciferase activity is restored. We demonstrated quantitative sensing of caspase-3 activities in living cells upon extracellular stimuli. Furthermore, the indicator enabled noninvasive imaging of the time-dependent caspase-3 activities in living mice. This cyclic luciferase indicator provides a general means for understanding the mechanism of physiological proteolytic processes and for screening novel pharmacological chemicals among candidates in living subjects.

References

1) T. Ozawa, Y. Natori, M. Sato and Y. Umezawa, *Nat. Methods* **4**, 413–419 (2007).
2) A. Kanno, T. Ozawa and Y. Umezawa, *Anal. Chem.* **78**, 8076–8081 (2006).
3) S. B. Kim, A. Kanno, T. Ozawa, H. Tao and Y. Umezawa, *ACS Chem. Biol.* **2**, 484–492 (2007).
4) A. Kanno, Y. Yamanaka, H. Hirano, Y. Umezawa and T. Ozawa, *Angew. Chem., Int. Ed.* **46**, 7595–7599 (2007).

Heterogeneous Catalytic Systems for Organic Chemical Transformations in Water

Department of Life and Coordination-Complex Molecular Science
Division of Complex Catalysis

UOZUMI, Yasuhiro	Professor
YAMADA, Yoichi M. A.	Assistant Professor
OE, Yohei	IMS Fellow
SUZUKA, Toshimasa	Post-Doctortal Fellow
KIMURA, Tsutomu	Post-Doctortal Fellow
MINAKAWA, Maki	Post-Doctortal Fellow
MATSUURA, Yutaka	Post-Doctortal Fellow
TAKENAKA, Hiroe	Research Fellow
TORII, Kaoru	Research Fellow
ARAKAWA, Takayasu	Graduate Student
BEPPU, Tomohiko	Graduate Student
SASAKI, Tokiyo	Secretary
HIGASHIBAYASHI, Azumi	Secretary
TANIWAKE, Mayuko	Secretary

Various organic molecular transformations catalyzed by transition metals were achieved under heterogeneous aqueous conditions by use of amphiphilic resin-supported metal complexes or metal nanoparticles which were designed and prepared by this research group. In particular, highly stereoselective asymmetric allylic substitutions and aerobic alcohol oxdation, both of which were performed in water under heterogeneous conditions with high recyclability of the polymeric catalysts, are highlights among the achievements of the 2006–2007 period to approach what may be considered ideal chemical processes of next generation. Representative results are summarized hereunder.

1. Nanometal Particle Catalysts Dispersed in Amphiphilic Resin Supports[1,2)]

An amphiphilic polystyrene-polyethylene glycol (PS-PEG) resin-dispersion of nanoparticles of platinum (ARP-Pt) was developed which had a mean diameter of 5.9 nm with a narrow size distribution throughout the resin (Scheme 1). ARP-Pt was found to be a useful and readily recyclable catalyst for aerobic oxidation of a wide variety of alcohols, including non-activated aliphatic and alicyclic alcohols, in water with an oxygen or air atmosphere under heterogeneous conditions to meet green chemical requirements. A PS-PEG resin-dispersion of nanopalladium catalyst was also prepared which catalyzed aerobic oxidation of alcohols and hydrodechlorination of aryl halides under heterogeneous aqueous conditions.

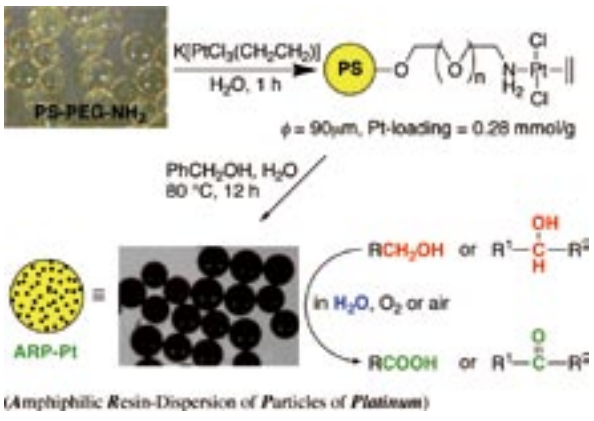

Scheme 1. Catalytic Aerobic Oxidation of Alcohols in Water with Amphiphilic Resin-Dispersion of Nanoparticles of Platinum.

2. Chiral Palladium Complexes Immobilized with Amphiphilic Resin Supports[3,4)]

Stereoselective polymeric palladium catalysts supported on an amphiphlic polystyrene-poly(ethylene glycol) (PS-PEG) resin were developed to realize asymmetric allylic substitutions in water under heterogeneous conditions. A polymeric (*R*)-2-(diphenylphosphino)binaphthyl (MOP) ligand anchored onto the PS-PEG resin by an (*S*)-alanine tether unit was identified through the library-based screening to be an effective chiral ligand for the asymmetric palladium-catalyzed π-allylic substitution of 1,3-diphenylpropenyl acetate with malonate nucleophiles under heterogeneous aqueous conditions. Nitromethane was safely applied as a C1 nucleophile for palladium-catalyzed

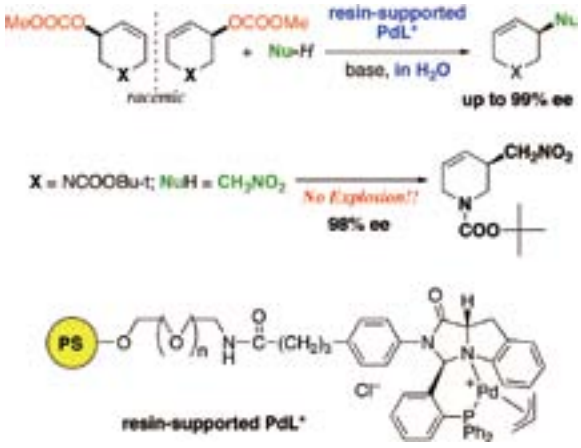

Scheme 2. Catalytic Asymmetric Allylic Substitution of Cycloalkenyl Esters in Water with an Amphiphilic Polymeric Chiral Palladium Complex.

π-allylic substitution of cyclic allylic substrates in water with amphiphilic PS-PEG resin-supported chiral imidazoindole-phosphine-palladium complexes (Scheme 2). Catalytic asymmetric nitromethylation of cycloalkenyl esters was achieved in water as a single reaction medium under heterogeneous conditions using 5 mol% palladium of a PS-PEG resin-supported palladium-imidazoindolephosphine complex to give optically active (cycloalkenyl)nitromethanes with up to 98% ee.

3. Self-Organized Polymeric Metal Complexes[5,6,7)]

A novel solid-phase 3D metal-organic coordination network catalyst was prepared *via* self-assembly from $PdCl_2$ $(CH_3CN)_2$ and a trisphosphine hub with three flexible alkyl-chain linkers. This insoluble network complex efficiently catalyzed the Suzuki-Miyaura reaction under atmospheric conditions in water. This catalyst was reused without loss of catalytic activity. A novel solid-phase self-organized catalyst of palladium nanoparticles was also prepared from $PdCl_2$ with main-chain viologen polymers *via* ionic convolution and reduction. This insoluble nanocatalyst nano-Pd-Viologen efficiently promoted α-alkylation of ketones with primary alcohols in the presence of $Ba(OH)_2 \cdot H_2O$ under atmospheric conditions without organic solvents. The nano-Pd-Viologen catalyst was reused without loss of catalytic activity. The both concepts of network complexation and ionic convolution are depicted in Scheme 3.

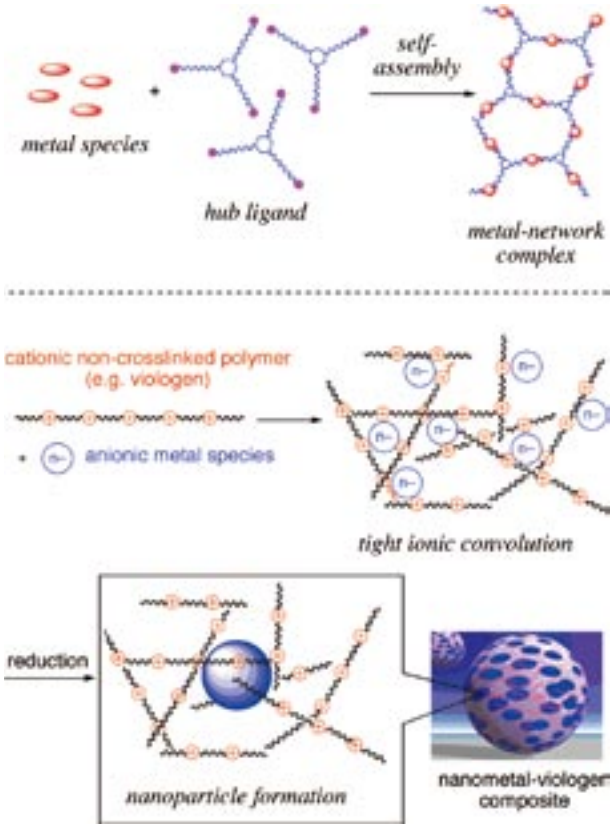

Scheme 3. Concepts of Self-Organized Network Complexation and Ionic Convolution.

4. Microchannel Reactor with a Catalytic Membrane[8)]

Instantaneous catalytic carbon–carbon bond forming reactions were achieved in a microchannel reactor having a polymeric palladium complex membrane (Scheme 4). The catalytic membrane was constructed inside the microchannel *via* self-assembling complexation at the interface between the organic and aqueous phases flowing laminarly, where non-crosslinked polymer-bound phosphine and ammonium tetrachloropalladate dissolved, respectively. Palladium-catalyzed coupling reaction of aryl halides and arylboronic acids was performed using the microchannel reactor to give quantitative yields of biaryls within 4 seconds of retention time in the defined channel region.

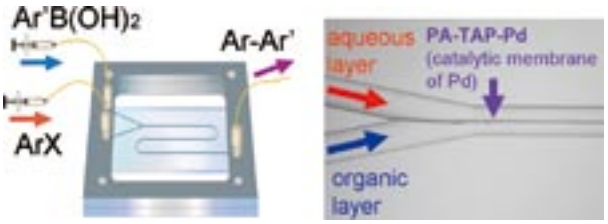

Scheme 4.

References

1) Y. M. A. Yamada, T. Arakawa, H. Hocke and Y. Uozumi, *Angew. Chem., Int. Ed.* **46**, 704–706 (2007).
2) Y. Uozumi, R. Nakao and H. Rhee, *J. Organomet. Chem.* **692**, 420–427 (2007).
3) Y. Kobayashi, D. Tanaka, H. Danjo and Y. Uozumi, *Adv. Synth. Catal.* **348**, 1561–1566 (2006).
4) Y. Uozumi and T. Suzuka, *J. Org. Chem.* **71**, 8644–8646 (2006).
5) Y. M. A. Yamada, Y. Maeda and Y. Uozumi, *Org. Lett.* **8**, 4259–4262 (2006).
6) Y. M. A. Yamada and Y. Uozumi, *Org. Lett.* **8**, 1375–1378 (2006).
7) Y. M. A. Yamada, H. Guo and Y. Uozumi, *Org. Lett.* **9**, 1501–1504 (2007).
8) Y. Uozumi, Y. M. A. Yamada, T. Beppu, N. Fukuyama, M. Ueno and T. Kitamori, *J. Am. Chem. Soc.* **128**, 15994–15995 (2006).

Awards

UOZUMI, Yasuhiro; Chemical Society of Japan Award for Creative Research.
UOZUMI, Yasuhiro; Green-Sustainable Chemistry Award and MEXT Minister Award for Green-Sustainable Chemistry.
YAMADA, Yoichi M. A.; Thieme Journal Award.

Metal Complexes Aiming Conversion between Chemical and Electrical Energies

Department of Life and Coordination-Complex Molecular Science
Division of Functional Coordination Chemistry

TANAKA, Koji	Professor
WADA, Tohru	Assistant Professor
OZAWA, Hironobu	IMS Fellow
KIMURA, Masahiro	Post-Doctoral Fellow
KOSHIYAMA, Tamami	Post-Doctoral Fellow
FUKUSHIMA, Takashi	Graduate Student
INOUE, Ayako	Graduate Student
YAMAGUCHI, Yumiko	Secretary
NAKAGAKI, Shizuka	Secretary

Metal ions involved in various metal proteins play key roles to generate metabolic energies through oxidation of organic molecules. Metal complexes having an ability to oxidize organic molecules at potentials more negative than that of reduction of dioxygen, therefore, are feasible catalysts to convert chemical energy to electrical one when combined with dioxygen reduction. Aqua-Ru complexes can be converted to high valent Ru=O ones by sequential proton and electron loss, and the some of the latter can oxidize organic molecules. However, the redox potentials to generate high valent Ru=O complexes are too positive to use as energy converters. We have succeeded smooth conversion from aqua to oxo ligands on Ru-dioxolene framework through proton coupled intramolecular electron transfer from the deprotonated from of Ru–OH species to dioxolene ligand. The aqua-oxo conversion using the unique redox behavior of Ru-dioxolene frameworks enabled to isolate unprecedented metal–oxo and –amino radical complexes. We are elucidating the reactivity of those complexes as electrocatalysts toward the oxidation of hydrocarbons.

1. Experimental and Theoretical Evaluation of the Charge Distribution over Ruthenium and Dioxolene Framework of [Ru(OAc)-(dioxolene)(terpy)] (terpy = 2,2':6',2"-terpyridine) Depending on Substituents[1)]

Ru complexes [Ru(OAc)(dioxolene)(terpy)] having various substituents on the dioxolene ligand (dioxolene = 3,5-*t*-$Bu_2C_6H_2O_2$ (**1**), 4-*t*-$BuC_6H_3O_2$ (**2**), 4-$ClC_6H_3O_2$ (**3**), 3,5-$Cl_2C_6H_2O_2$ (**4**), $Cl_4C_6O_2$ (**5**); terpy = 2,2':6'2"-terpyridine) were prepared. EPR spectra of these complexes in glassy frozen solutions (CH_2Cl_2:MeOH = 95:5, vol./vol.) at 20 K showed anisotropic signals with g tensor components 2.242 > g_1 > 2.104, 2.097 > g_2 > 2.042, and 1.951 > g_3 > 1.846. An anisotropic value, $\Delta g = g_1 - g_3$, and an isotropic g value, $\langle g \rangle = [(g_1^2 + g_2^2 + g_3^2)/3]^{1/2}$, increase in the order **1** < **2** < **3** < **4** < **5**. The resonance between the Ru^{II}(sq) (sq = semiquinone) and Ru^{III}(cat) (cat = catecholato) frameworks shifts to the latter with an increase of the number of electron-withdrawing substituents on the dioxolene ligand. DFT calculations of **1**, **2**, **3**, and **5** also support the increase of the Ru spin density (Ru^{III} character) with an increase of the number of Cl atoms on the dioxolene ligand. The singly occupied MOs (SOMOs) of **1** and **5** are very similar to each other and stretch out the Ru–dioxolene frameworks, whereas the LUMO of **5** is localized on Ru and two O atoms of dioxolene in comparison with that of **1**. Electron-withdrawing groups decrease the energy levels of both the SOMO and LUMO. An increase in the number of Cl atoms in the dioxolene ligand results in an increase of the positive charge on Ru. Successive shifts in the electronic structure between the Ru^{II}(sq) and Ru^{III}(cat) frameworks caused by the variation of the substituents are compatible with the experimental data (Figure 1).

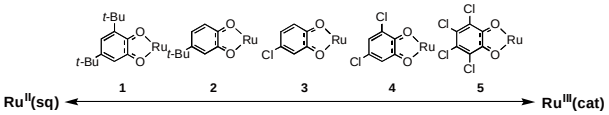

Figure 1. Charge distribution on the Ru–dioxolen framework depending on substituents.

2. Generation of Ru^{II}–Semiquinone–Anilino Radical through Deprotonation of Ru^{III}–Semiquinone–Anilido Complex[2)]

Aminyl radicals are thermodynamically unstable and have an ability to oxidize organic substrates through H-atom abstraction. Metal complexes bearing an aminyl radical may, therefore, have potential uses as new oxidation catalysts in organic synthesis. Actual electronic states of aminyl radical metal

complexes would lie somewhere between two limiting resonance structures such as the amido state $\{M^{(n+1)+}–NR_2\}$ and the aminyl radical $\{M^{n+}–^{\bullet}NR_2\}$ and would usually be shifted toward the former. Recently, metal complexes having aminyl radicals were isolated by means of chemical and electrochemical oxidation of the corresponding metal amido complexes. On the other hand, a Ru^{II}–semiquinone–oxyl radical complex, $[Ru^{II}(terpy)(Bu_2sq)(O^{\bullet-})]$ (terpy = 2,2':6',2"-terpyridine, Bu_2sq^- = 3,5-di-*tert*-butylsemi- quinonate), was isolated through deprotonation of $[Ru^{III}(terpy)(Bu_2sq)(OH)]^+$ under basic conditions without using any oxidants. Furthermore, the deprotonated species of $[Ru^{III}(terpy)(Bu_2sq)(NH_3)]^{2+}$ and $[Ru^{III}(NH_2\text{-bpa})(Bu_2sq)]^{2+}$ (NH_2-bpa = bis(2-pyridylmethyl)-2-aminoethylamine) were proved to oxidize alcohols to aldehydes or ketones with the generation of $[Ru^{II}(terpy)(Bu_2sq)(NH_3)]^+$ and $[Ru^{II}(NH_2\text{-bpa})(Bu_2sq)]^+$, respectively. The most plausible active species for the oxidation of alcohols is a Ru^{II}–semiquinone–aminyl radical that is a limiting resonance structure of an Ru^{III}–semiquinone–amido complex. Although the Ru^{II}–semiquinone–aminyl radical intermediate was too labile to identify its existence in oxidation reactions, an analogous Ru^{III}–semiquinone–anilino radical complex that also would be formed from the corresponding Ru^{III}–semiquinone–aniline complexes may be stabilized due to the π-conjugated system of aniline group. We successfully isolated the Ru^{II}–semiquinone–anilino radical, $[Ru^{II}(^{\bullet}NPh\text{-}bpa)(Bu_2sq)]\text{-}2H_2O$ (**2**), and its one-electron reduced species, *i.e.*, the Ru^{II}–catechol–anilino radical, $[Ru^{II}(^{\bullet}NPh\text{-}bpa)(Bu_2cat)]^-$ (**3**), complexes bearing the 2-[Bis(2-pyridylmethyl) aminomethyl]-anilido ligand ($NPh\text{-}bpa^{2-}$). The anilino radical characters of **2** and **3** are proved by EPR spectroscopy, resonance Raman spectroscopy, and DFT calculations (Figure 2).

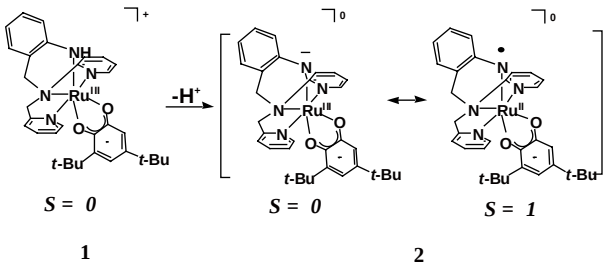

Figure 2. The formation of anilino radical complex.

3. Proton Coupled Electron Transfer Driven by the Acid-Base Equilibrium of Aqua–Ruthenium–Dioxolene Complexes

Ruthenium–dioxolene complexes with an aqua ligand, $[Ru^{III}(trpy)(R_l\text{-dioxolene})(OH_2)](ClO_4)_2$ (R_1 = Bu_2 ([**6**]$(ClO_4)_2$), Bu ([**7**]$(ClO_4)_2$), Cl ([**8**]$(ClO_4)_2$), and $[Ru^{III}(trpy)(R_2\text{-dioxolene})(OH_2)](BF_4)$ (R_2 = Cl_2 (**9**) and Cl_4 (**10**)) were prepared by the hydrolysis of the correspondent acetato complexes, $Ru^{III}(trpy)(R_3\text{-dioxolene})(OAc)$ (R_3 = Bu_2 (**1**), Bu (**2**), Cl (**3**), Cl_2 (**4**) and Cl_4 (**5**)). The EPR spectra of ruthenium-acetato complexes, suggest that the Ru^{III}(SQ) framework is the principal contribution to the electronic structure of the complexes, **1**–**3**, whereas the Ru^{III}(Cat) one became the main contribution to the complexes **4** and **5**. The electronic structures of the analogous aqua complexes are also largely influenced by the substituents of the dioxolene ligand. The dicationic complexes [**6**]$(ClO_4)_2$, [**7**]$(ClO_4)_2$, and [**8**]$(ClO_4)_2$ have the Ru^{III}(SQ) frameworks. The acid-base reaction of the aqua ligand of $[\mathbf{7}]^{2+}$, whose redox potentials lied between those of $[\mathbf{6}]^{2+}$ and $[\mathbf{8}]^{2+}$, proceeds *via* two subsequent proton dissociations. The CVs of those complexes also indicate the formation of oxyl radical complexes $[Ru^{II}(trpy)(SQ)(O^{-\bullet})]^0$, because addition of two equivs of BuOK to $[Ru^{III}(trpy)(SQ)(OH_2)]^{2+}$ resulted in shift of the rest potential of the solution to negative directions across the $Ru^{III}(SQ)/Ru^{II}(SQ)$ redox potential. On the other hand, the aqua complexes $[\mathbf{9}]^+$ and $[\mathbf{10}]^+$ that have mainly the Ru^{III}(Cat) character due to more electron-withdrawing dioxolene ligands dissociate only one proton in the experimental conditions. The CV did not show the formation of the Ru^{II}(Cat) core by an addition of large excess of BuOK to $[Ru^{III}(SQ)(trpy)(OH_2)]^{2+}$. It is, therefore, concluded that the conversion from $[Ru^{III}(SQ)(trpy)(OH^-)]^+$ to $[Ru^{II}(SQ)(trpy)(O^{-\bullet})]^0$ through $[Ru^{III}(SQ)(trpy)(O^{2-})]^0$ is achieved by the neutralization energy generated by treatment of the Ru–OH bond with BuOK, whereas it is not enough to convert from $[Ru^{III}(SQ)(trpy)(OH^-)]^+$ to $[Ru^{II}(Cat)(O^{-\bullet})]^0$ *via* $[Ru^{III}(SQ)(trpy)(O^{2-})$ $[Ru^{III}(SQ)(trpy)(O^{2-})]^0$.

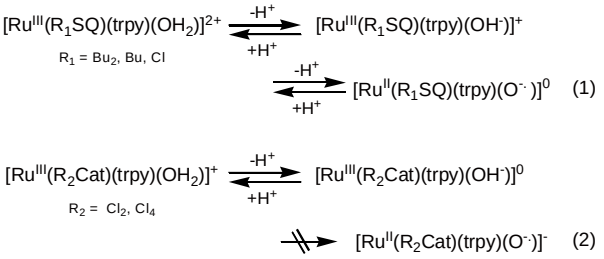

References

1) T.Wada, M.Yamanaka, T. Fujihara, Y. Miyazato and K. Tanaka, *Inorg. Chem.* **45**, 8887–8894 (2006).

2) Y. Miyazato, T. Wada, K. Tanaka, E. Fuhita and J. T. Muckerman, *Angew. Chem., Int. Ed.* **46**, 5728–5730 (2007).

Synthesis and Reactions of Transition Metal Complexes Having Aryloxide-Based Ligands, Especially with Regard to Activation of Small Molecules

Department of Life and Coordination-Complex Molecular Science
Division of Functional Coordination Chemistry

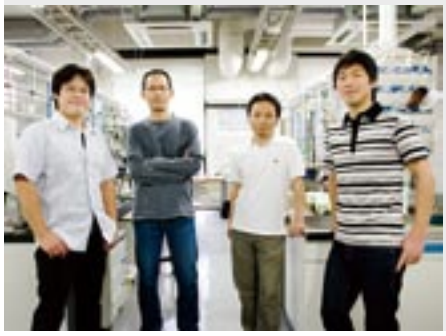

KAWAGUCHI, Hiroyuki	Associate Professor
MATSUO, Tsukasa	Assistant Professor*
WATANABE, Takahito	IMS Fellow
AKAGI, Fumio	Post-Doctoral Fellow
ARII, Hidekazu	Post-Doctoral Fellow
FUKAWA, Tomohide	Post-Doctoral Fellow
ISHIDA, Yutaka	Post-Doctoral Fellow

This project is focused on the design and synthesis of new ligands that are capable of supporting novel structural features and reactivity. Currently, we are investigating multidentate ligands based on aryloxide and thiolate. In addition, we set out to study metal complexes with sterically hindered aryloxide and arylthiolate ligands. Our recent efforts have been directed toward activation of small molecules.

Development of ligands that play important roles in coordination chemistry has been the subject of intense interest. The chemistry of metal aryloxide complexes has shown that aryloxide ligands can promote various important transformations at metal centers. Therefore, aryloxide ligands complement the well-studied cyclopentadienyl-based systems, with the major difference being the greater reactivity of the aryloxide complexes due to their relatively higher unsaturation and lower coordination numbers for a $(ArO)_nM$ fragment. However, coordinatively unsaturated metal complexes undergo facile ligand redistribution reactions, which are occasionally a severe obstacle to synthetic efforts.

One of strategies for overcoming this problem is the use of covalently linked ancillary ligands, thereby limiting ligand mobility and leaving little possibility to reorganize the molecule. This feature has led to the isolation and structural characterization of a number of metal complexes that are difficult to obtain with aryloxide monodentate ligands. In this context, we set out to investigate aryloxide-based multidentate ligands as new ancillary ligands.

1. Reduction of Carbon Dioxide with Hydrosilanes Catalyzed by Zirconium-Borane Complexes[1)]

Carbon dioxide is the stable carbon end product of metabolism and other combustions, and it is an abundant yet low-value carbon source. This molecule would be very valuable as a renewable source if it were to be effectively transformed into reduced organic compounds under mild conditions. However, thermodynamic stability of CO_2 has prevented its utilization in industrial chemical processes, and thus this represents a continuing scientific challenge. In this study, we found that CO_2 is catalytically converted into CH_4 and siloxanes via bis(silyl)acetals with a mixture of a zirconium benzyl phenoxide complex and tris(pentafluorophenyl)borane ($B(C_6F_5)_3$).

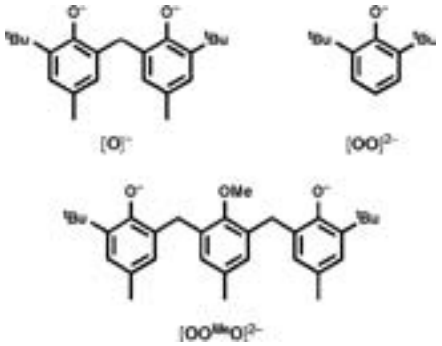

Scheme 1.

In a first set of experiments, we studied the catalytic activity of cationic zirconium benzyl complexes bearing phenoxide ligands (Scheme 1) in the course of reducing CO_2 with $PhMe_2SiH$ as the test substrate. The catalysts used in this study were synthesized by treatment of the dibenzyl complexes with $B(C_6F_5)_3$ in toluene. The reaction of CO_2 with $PhMe_2SiH$ proceeded exothermically to form $(PhMe_2Si)_2O$ (Scheme 2). Performing the analogous reaction in benzene-d_6 in a NMR tube revealed the release of CH_4 as the byproduct. The resonance due to CH_4 was observed as singlet at 0.15 ppm in the ^1H NMR spectrum. Mono- and bis-phenoxide ligands $[\mathbf{O}]^-$ and $[\mathbf{OO}]^{2-}$ gave zirconium complexes that preformed with low activity relative to the tridentate ligand $[\mathbf{OO^{Me}O}]^{2-}$. The combination of a zirconium complex with $B(C_6F_5)_3$ is responsible

for this result, because the analogous reaction using [(**OO^{Me}O**)Zr(CH_2Ph)][$B(C_6F_5)_4$] did not give CH_4 but led to formation of Ph_2Me_2Si and Me_2SiH_2. Thus, neither zirconium cationic species nor $B(C_6F_5)_3$ alone provided an active catalyst.

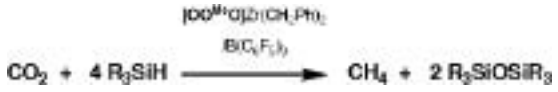

Scheme 2.

In order to obtain insight into the intervening processes in the reaction, isotopically enriched $^{13}CO_2$ (99 atom% ^{13}C) was admitted into a resealable NMR tube containing a solution of (**OO^{Me}O**)Zr(CH_2Ph)$_2$, $B(C_6F_5)$, and Et_3SiH in benzene-d_6 at room temperature. The reaction requires approximately one week for completion and is monitored by NMR spectroscopy. The reaction proceeded cleanly, during which time $^{13}CO_2$ and Et_3SiH were fully consumed. Monitoring the reaction by $^{13}C\{^1H\}$ NMR spectroscopy indicates the presence of bis(silyl)acetal $^{13}CH_2(OSiEt_3)_2$ as a detectable intermediate. The resonance at 84.5 ppm due to $^{13}CH_2(OSiEt_3)_2$ grew to a maximum relative intensity over a period of about 7 h and then decreased as that at –4.4 ppm due to $^{13}CH_4$ continued to grow until, after about 1 week, it was the only resonance attributable to a ^{13}C–labeled product. Additionally, in the absence of proton decoupling, the resonances due to $^{13}CH_2(OSiEt_3)_2$ and $^{13}CH_4$ split into a triplet and a quintet with a coupling constant of 161.5 and 125.6 Hz, respectively. This observation unambiguously confirms that the carbon atom of CH_4 originates from CO_2, and the source of its hydrogen atoms is added Et_3SiH.

The method for catalytic reduction of CO_2 presented here offers some significant advantages, since it proceeds under mild conditions and permits complete reduction of CO_2 to CH_4. Another curious aspect of this system is the formation of polysiloxane from CO_2 and hydrosilane in chemical CO_2 fixation. The present results are promising, but we note that catalytic activity will need to be improved and the long-term stability and performance of the catalyst demonstrated.

2. Zirconium Complexes of a Tridentate Bis(aryloxide)-NHC Ligand[2)]

The chemistry and application of *N*-heterocyclic carbenes (NHCs) have been extensively explored. They can bind as two-electron donors to a wide range of transition metal, main group, and f-block derivatives. Especially, NHCs have been found extensive use as ancillary ligands in late transition metal complexes, in which they have shown enhanced catalytic activity compared to their phosphine analogues. In contrast, NHC complexes of early transition metals are considerably less developed despite the great potential of this class of molecules. This is mainly due to the ease of dissociation of the NHC ligand from the electron deficient metal center, which makes it difficult to study the chemistry of NHCs in early transition metals and f-elements. A potential means of directing metal–NHC interactions is the covalent tethering of the anionic functional groups to the NHC ligand system, where the NHC moiety is held in proximity of the metal center by a covalent tether and should affect reactivity in a specific way. In this study, we show the synthesis of zirconium complexes having a bis(aryloxide)-NHC ligand ([**OCO**]$^{2-}$, Scheme 3)

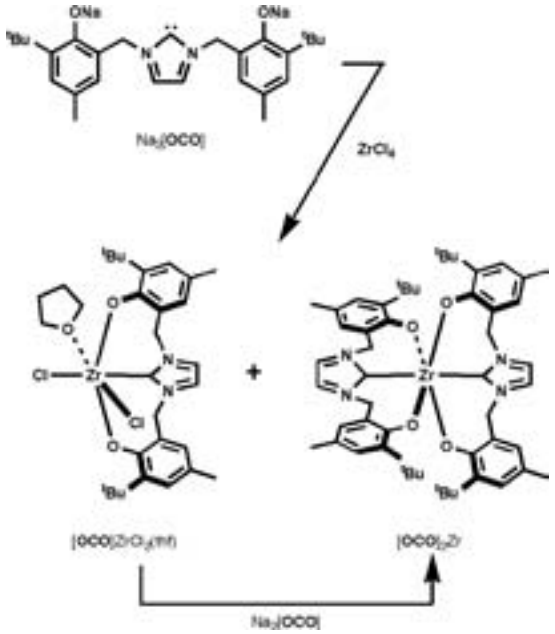

Scheme 3.

The disodium salt of a ligand Na_2[**OCO**], was prepared by reaction of H_3[**OCO**]Br with 3 equiv of $NaN(SiMe_3)_2$. Reaction of $ZrCl_4(thf)_2$ with 1 equiv of Na_2[**OCO**] gave a mixture of [**OCO**]$ZrCl_2$(thf) and [**OCO**]$_2$Zr. When the amount of Na_2[**OCO**] was increased to 2 equiv, [**OCO**]$_2$Zr was obtained in good yield. The complex [**OCO**]$ZrCl_2$(thf) is a precursor to organometallic derivatives, and treatment with $PhCH_2MgCl$ or Me_3SiCH_2Li yielded [**OCO**]ZrR_2 (R = CH_2Ph, CH_2SiMe_3). The disodium salt Na_2[**OCO**] is unstable and undergoes 1,2-benzyl migration, while zirconium complexes of the [**OCO**]$^{2-}$ ligand are found to be thermally stable in solid and solution.

Compounds [**OCO**]$ZrCl_2$(thf) and [**OCO**]ZrR_2 should provide excellent starting materials for investigation of the reactivity of this class of group 4 metal complexes. We expect it to demonstrate a rich and varied chemistry.

References

1) T. Matsuo and H. Kawaguchi, *J. Am. Chem. Soc*. **128**, 12362–12363 (2006).

2) D. Zhang, H. Aihara, T. Watanabe, T. Matsuo and H. Kawaguchi, *J. Organomet. Chem*. **692**, 234–242 (2007).

* Present Address; RIKEN Wako Institute, Frontier Research System

Visiting Professors

Visiting Professor
KITAGAWA, Hiroshi *(from Kyushu University)*

Creation of Novel Functional Nano Materials Based on Proton-Coupled Electronic Properties

Dynamics of molecules and ions in "coordination nano-space" are acted by characteristic nano-fields such as intermolecular interaction, coulomb interaction, catalytic action, *etc*. This project is to reveal a basic principle of an unusual nano-field acting on coordination space, and to create the nano space where the energy conversions can be easily operated. In particular, we aim at the construction of coordination nano space system which is able to control a series of energy operations such as generation, separation, storage, material conversion of an energy molecule H_2, or electron/ion transport. In this year, we have explored a novel hydrogen-energy functional coordination nano-space by using proton-coupled redox and electron-proton interaction. In the present project, we will create new 1) hydrogen-storage nano-materials, 2) highly proton-conductive coordinatiom polymers, 3) highly electron-proton conductive matrerials, *etc*.

Visiting Associate Professor
KANAMORI-KATAYAMA, Mutsumi *(from RIKEN)*

Development of the Assay System for Protein-RNA Interactions

Recently, it has been cleared that a large amount of non-coding RNA (ncRNA) existed in mammalian cells. Though some ncRNAs are analyzed and cleared to have important functions, what most ncRNAs do is largely unknown. These ncRNAs are thought to function with Protein, RNA or DNA rather than by themselves. Therefore, it is thought that the information of interactions will play an important role to annotate the function of ncRNAs.

So, we focused on the protein-RNA interaction (PRI), and have been developing the assay system to obtain PRI information efficiently.

Visiting Associate Professor
KONDO, Mitsuru *(from Shizuoka University)*

Synthesis of Coordination Polymers with Metallocene Units

Network materials obtained by connections of metallocene units with organic components have attracted intense attentions toward the developments of new functional materials because of the high redox properties and versatile flexibilities based on the metallocene units. Nevertheless, assembled materials with metallocene units excepting ferrocene moieties are still limited. We have prepared the coordination polyerms with cobaltocene and rhodocene units. Reccently, we have selected ruthenocene-1,1'-dicarbocxylic acid (H_2rudc) toward creations of new network materials with ruthenocene units, and have succeeded in syntheses and characterizations of two new network materials, (dpe)(H_2rudc) (dpe = bipyridylethyelene) (**1**) and (Hdpp)(Hrudc) (dpp = dipyridylpropane) (**2**). The effects of the free rotations of the Cp rings on the network structures have been shown by their structural characterizations. That is, although both compounds **1** and **2** give linear networks constructed by intermolecular hydrogen bonds, compound **2** demonstrates a quite unique folding structure compared to the simple linear structure of **1**.